J. Membrane Biol. 190, 57–73 (2002)
DOI: 10.1007/s00232-002-1024-6

The Journal of
Membrane
Biology

Presteady-State and Steady-State Kinetics and Turnover Rate of the Mouse γ-Aminobutyric Acid Transporter (mGAT3)

A. Sacher[1], N. Nelson[1], J.T. Ogi[2], E.M. Wright[3], D.D.F. Loo[3], S. Eskandari[2]
[1]Department of Biochemistry, The George S. Wise Faculty of Life Sciences, Tel Aviv University, Tel Aviv 69978, Israel
[2]Biological Sciences Department, California State Polytechnic University, 3801 West Temple Ave., Pomona, CA 91768-4032, USA
[3]Department of Physiology, School of Medicine, University of California, Los Angeles, CA 90095-1751, USA

Received: 8 April 2002/Revised: 9 July 2002

Abstract. We expressed mouse γ-aminobutyric acid (GABA) transporter (mGAT3) in *Xenopus laevis* oocytes and examined its steady-state and presteady-state kinetics and turnover rate by using tracer flux and electrophysiological methods. In oocytes expressing mGAT3, GABA evoked a Na^+-dependent and Cl^--facilitated inward current. The dependence on Na^+ was absolute, whereas that for Cl^- was not. At a membrane potential of −50 mV, the half-maximal concentrations for Na^+, Cl^-, and GABA were 14 mM, 5 mM, and 3 μM. The Hill coefficient for GABA activation and Cl^- enhancement of the inward current was 1, and that for Na^+ activation was ≥2. The GABA-evoked inward current was directly proportional to GABA influx (2.2 ± 0.1 charges/GABA) into cells, indicating that under these conditions, there is tight ion/GABA coupling in the transport cycle. In response to step changes in the membrane voltage and in the absence of GABA, mGAT3 exhibited presteady-state current transients (charge movements). The charge-voltage (Q-V) relation was fitted with a single Boltzmann function. The voltage at half-maximal charge ($V_{0.5}$) was +25 mV, and the effective valence of the moveable charge ($z\delta$) was 1.6. In contrast to the ON transients, which relaxed with a time constant of ≤30 msec, the OFF transients had a time constant of 1.1 sec. Reduction in external Na^+ ($[Na^+]_o$) and Cl^- ($[Cl^-]_o$) concentrations shifted the Q-V relationship to negative membrane potentials. At zero $[Na^+]_o$ (106 mM Cl^-), no mGAT3-mediated transients were observed, and at zero $[Cl^-]_o$ (100 mM Na^+), the charge movements decreased to ≈30% of the maximal charge (Q_{max}). GABA led to the elimination of charge movements. The half-maximal concentrations for Na^+ activation, Cl^- enhancement, and GABA elimination of the charge movements were 48 mM, 19 mM, and 5 μM, respectively. Q_{max} and I_{max} obtained in the same cells yielded the mGAT3 turnover rate, 1.7 sec^{-1} at −50 mV. The low turnover rate of mGAT3 may be due to the slow return of the empty transporter from the internal to the external membrane surface.

Key words: GABA — Mouse GAT3 — Charge movement — Chloride dependence — Neurotransmitter transporter

Introduction

Transport of the inhibitory neurotransmitter γ-aminobutyric acid (GABA) into cells is accomplished by Na^+- and Cl^--dependent GABA transporters (GATs) found in the plasma membrane of neurons and glia (Borden, 1996; Nelson, 1998). The GABA transporters are responsible for maintaining the fidelity of GABAergic synaptic neurotransmission in the central nervous system and, hence, their activity can influence a variety of physiological (e.g., inhibitory neurotransmission) as well as pathophysiological (e.g., epileptic seizures) states (Borden, 1996; Roettger & Amara, 1999). Four mammalian GABA transporter isoforms have been cloned from mouse, rat, canine, and human tissues (Guastella et al., 1990; Nelson, Mandiyan & Nelson, 1990; Borden, 1996; Borden et al., 1992, 1994, 1995; Clark et al., 1992; Liu et al., 1992, 1993; López-Corcuera et al., 1992; Yamauchi et al., 1992; Nelson, 1998). The mouse isoforms have been labeled GAT1–GAT4, whereas the

Correspondence to: S. Eskandari; email: seskandari@csupomona.edu

rat, canine, and human homologues are referred to as GAT-1, GAT-2, and GAT-3. The fourth isoform is a hypertonicity-regulated betaine/GABA transporter (BGT-1) (Yamauchi et al., 1992). Rat and human GAT-1, BGT-1, GAT-2, and GAT-3 are the homologues of mouse GAT1, GAT2, GAT3, and GAT4, respectively (for review, *see* Borden, 1996).

Functional examinations of the GABA transporters have disproportionately favored the GAT-1 isoform (Mager et al., 1993, 1996; Cammack, Rakhilin & Schwartz, 1994; Lu et al., 1995; Cammack & Schwartz, 1996; Lu & Hilgemann, 1999a,b; Li, Farley & Lester, 2000; Loo et al., 2000; Forlani et al., 2001a), as well as to some extent the canine BGT-1 (Yamauchi et al., 1992; Matskevitch et al., 1999; Forlani et al., 2001b). These studies have indicated that GAT1 and GAT2/BGT-1 perform different functions in vivo. It is thought that GAT1 functions to clear the synapse of presynaptically released GABA, whereas GAT2/BGT-1 is involved in osmoregulation in the central nervous system, as well as in other organs (e.g., kidney). In addition, functional studies of GAT1 and GAT2/BGT-1 have demonstrated differences with respect to ion/GABA stoichiometry, and different mechanisms of cotransport have been proposed (Hilgemann & Lu, 1999; Matskevitch et al., 1999; Loo et al., 2000).

In light of the differences noted between GAT1 and GAT2/BGT-1, and in view of the primary sequence divergence of GAT3 and GAT4 from GAT1 and GAT2/BGT-1 (Reizer, Reizer & Saier, 1994; Lill & Nelson, 1998), it is imperative that the functional features of GAT3 and GAT4 be thoroughly examined. Here, we have used electrophysiological and tracer-uptake methods to carry out a comprehensive functional characterization of mouse GAT3 (mGAT3). Our results show that many novel functional features of mGAT3 distinguish it from GAT1 and GAT2/BGT-1, and provide insight into the mechanism of Na^+/Cl^-/GABA cotransport.

Materials and Methods

Cloning procedures

Mouse GAT3 was cloned as previously described (Liu et al., 1992, 1993; López-Corcuera et al., 1992). The cDNA was subcloned by PCR into pGEM-HJ plasmid (Liman Tytgat & Hess, 1992). This expression vector contains 5′ and 3′ untranslated regions from the *Xenopus* β-globin gene, which lead to improved message stability. mGAT3 was subcloned by PCR amplification from the original plasmid using the primers TAT CAT ATG GAG AAC AGG GCC TCG GGA AC and TAT ACT AGT TGT GAG CCT GAG AAG GGA TGT C that contain the *Nde*I and *Spe*I sites, respectively. Following digestion by these enzymes and blunt-end by fill-in, the fragment was cloned into the *Sma*I site of pGEM-HJ. The orientation was verified with several restriction enzymes and sequencing, and in the proper orientation the ATG, which starts the translation, was located 6 bases from the cloning site. Following linearization of the plasmid by *Not*I, cRNA was synthesized in vitro (Ambion mMessage mMachine; Austin, TX) using T7 RNA polymerase.

Expression of mGAT3 in *Xenopus* Oocytes

Xenopus laevis frogs were anesthetized in 0.1% tricaine methanesulfonate, small lobes of the ovary were removed, and the animals were sacrificed by an overdose of Nembutal (60 mg) in accordance with the protocol approved by the Animal Care and Use Committee at this institution. Stage V–VI oocytes were isolated from the ovary, and injected with cRNA for mouse GAT3 (Liu et al., 1993). Oocytes were maintained in Barth's medium (in mM: 88 NaCl, 1 KCl, 0.33 $Ca(NO_3)_2$, 0.41 $CaCl_2$, 0.82 $MgSO_4$, 2.4 $NaHCO_3$, 10 HEPES, pH 7.4, and 50 μg/ml gentamicin, 100 μg/ml streptomycin, and 100 units/ml penicillin) at 18°C for 2–14 days until used in experiments. All experiments were performed at 21 ± 1°C.

Experimental Solutions

Unless otherwise indicated, experiments were performed in a NaCl buffer containing (in mM): 100 NaCl, 2 KCl, 1 $CaCl_2$, 1 $MgCl_2$, 10 HEPES, pH 7.4. In Na^+-free solutions, NaCl was isosmotically replaced with choline-Cl. In Cl^--free solutions, NaCl was isosmotically replaced with either Na-gluconate or Na-[2-(N-morpholino)ethanesulfonic acid] (Na-MES), and KCl, $CaCl_2$, and $MgCl_2$ were replaced with the corresponding gluconate salts. Choline, gluconate, and MES have no effect on mGAT3 steady-state or presteady-state properties (*not shown*). GABA was added to the above solutions as indicated. All reagents were purchased from Sigma (St. Louis, MO).

GABA Uptake in *Xenopus* Oocytes

Control and mGAT3-expressing oocytes were incubated for 30 minutes in solutions containing various concentrations of GABA in addition to 22 nM of [^{3}H]-GABA (Amersham BioSciences; Piscataway, NJ). For uptake under voltage clamp (*see* Fig. 1*C*), the membrane potential was held at −50 mV, and the holding current was continuously monitored. Oocytes were initially incubated in the NaCl buffer until baseline was established. GABA (100 μM) and [^{3}H]-GABA (22 nM) were added to the perfusion solution for 5–10 minutes. At the end of the incubation period, GABA and the isotope were removed from the perfusion solution until the holding current returned to the baseline. The oocytes were removed from the experimental chamber, washed in ice-cold choline-Cl buffer, and solubilized in 10% sodium dodecyl sulfate. Oocyte [^{3}H]-GABA content was determined in a liquid scintillation counter (Beckman LS 5000CE; Fullerton, CA). Net inward charge was obtained from the time integral of the GABA-evoked inward current and correlated with GABA influx in the same cell (Eskandari et al., 1997; Mackenzie, Loo & Wright, 1998).

Electrophysiological Measurements and Data Analysis

The two-microelectrode voltage-clamp technique was used for the recording of whole-cell mGAT3-mediated currents. Oocytes were voltage clamped by using the Warner Oocyte Clamp (OC-725C; Warner Instrument Corporation; Hamden, CT). In the experimental chamber, oocytes were initially stabilized in a NaCl buffer, and the composition of the bath was changed as indicated. In Cl^--free experiments, the reference electrode was connected to the experimental oocyte chamber via an agar bridge (3% agar in 3 M

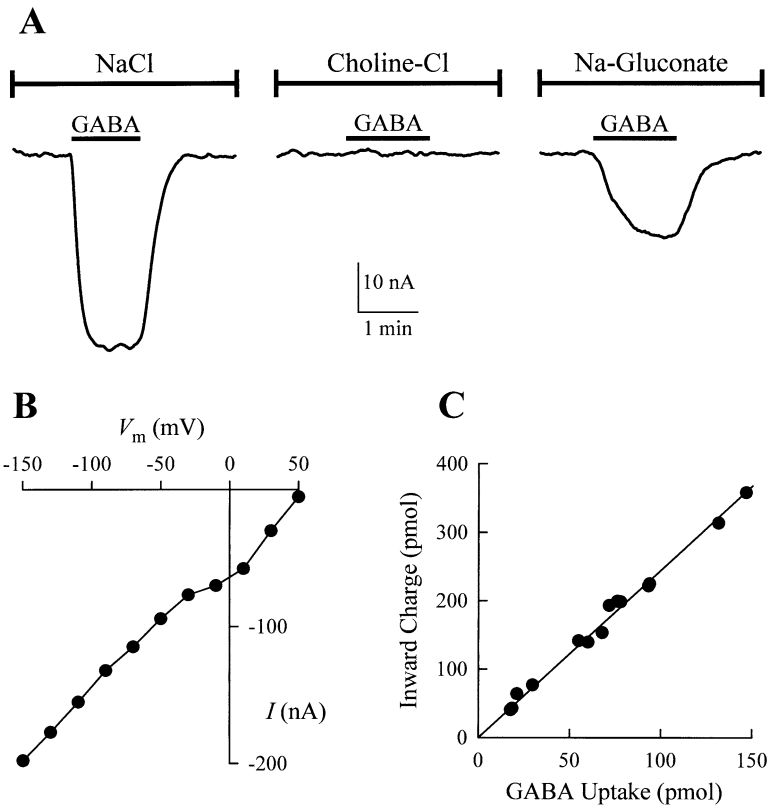

Fig. 1. Mouse GAT3 GABA transport is electrogenic. (*A*) Current traces from an mGAT3-expressing oocyte maintained at a holding potential of −50 mV. The response to addition of GABA (100 μM) was examined as the composition of the bathing medium was altered. In the presence of external Na^+ and Cl^- ($[Na^+]_o$ = 100 mM and $[Cl^-]_o$ = 106 mM; *left panel*), GABA induced an inward current of ≈40 nA in magnitude. In the absence of external Na^+ (choline-Cl replacement; *middle panel*), no GABA-evoked inward current was observed. In the absence of external Cl^- (Na-gluconate replacement; *right panel*), the GABA-evoked inward current was ≈50% of that in the presence of 106 mM Cl^-. In control oocytes, GABA does not induce a current (*not shown*). (*B*) The magnitude of the GABA-evoked current depended on the membrane potential (V_m); it tended toward zero at depolarizing potentials, and increased with hyperpolarizing potentials. The current-voltage (*I-V*) relationship was fairly linear in the voltage range tested (−150 mV to +50 mV). (*C*) The magnitude of the GABA-evoked inward current was directly proportional to GABA uptake. The ratio of net inward charge (time integral of the inward current) to GABA uptake obtained in the same cells was 2.2 ± 0.1 charges/GABA (N = 14). V_m was −50 mV.

KCl). For continuous holding-current measurements, currents were low-pass filtered at 1 Hz, and sampled at 10 Hz. Under these conditions, GABA-evoked currents as small as 1 nA could be resolved, although typical inward current levels ranged from 20–100 nA (at −50 mV).

To obtain steady-state current-voltage (*I-V*) relations, the pulse protocol (pCLAMP 8.1, Axon Instruments; Union City, CA) consisted of 300-msec voltage steps from a holding potential of −50 mV to a series of test voltages (V_m) from +50 to −150 mV in 20-mV steps. Currents were low-pass filtered at 500 Hz (LPF 8; Warner Instrument Corporation), and sampled at 2 kHz. Substrate-induced steady-state cotransporter currents were obtained from the difference between the steady-state currents in the absence and presence of GABA. At each membrane potential, the dependence of the steady-state currents on the extracellular substrate concentration ($[GABA]_o$, $[Na^+]_o$, and $[Cl^-]_o$) was determined by fitting the induced currents (I) to Equation 1:

$$I = \frac{I^S_{max}[S]^n}{(K^S_{0.5})^n + [S]^n} \quad (1)$$

where S is the substrate (GABA, Na^+, or Cl^-), I^S_{max} is the maximal substrate-induced current, $K^S_{0.5}$ is the substrate concentration at half I^S_{max} (half-maximal concentration), and n is the Hill coefficient.

To examine the carrier-mediated presteady-state current transients, the pulse protocol consisted of voltage jumps (200–400 msec) from the holding voltage (−50 mV) to test voltages ranging from +80 to −70, −110, or −130 mV in 10-mV steps. Unless otherwise indicated, voltage pulses were separated by an interval of at least 4 sec in order to allow for complete relaxation of the OFF transients (*see* Results). Currents were low-pass filtered at 1 kHz and sampled at 12.5 kHz without averaging. To obtain the transporter presteady-state currents, at each V_m, the total current, $I(t)$, was fitted to Equation 2:

$$I(t) = I_1 e^{-t/\tau_1} + I_2 e^{-t/\tau_2} + I_{SS} \quad (2)$$

where t is time, $I_1 e^{-t/\tau_1}$ is the oocyte capacitive transient current with initial value I_1 time constant τ_1, $I_2 e^{-t/\tau_2}$ is the transporter transient current with initial value I_2 and time constant τ_2, and I_{SS} is the steady-state current (Loo *et al.*, 1993). At each V_m, the total transporter-mediated charge (Q) was obtained by integration of the transporter transient currents. The charge-voltage (*Q-V*) relations obtained were then fitted to a single Boltzmann function (Equation 3):

$$\frac{Q - Q_{hyp}}{Q_{max}} = \frac{1}{1 + e^{[z\delta F(V_m - V_{0.5})/RT]}} \quad (3)$$

where $Q_{max} = Q_{dep} - Q_{hyp}$ (Q_{dep} and Q_{hyp} are Q at depolarizing and hyperpolarizing limits), z is the apparent valence of movable charge, δ is the fraction of the membrane electric field traversed by the charge, $V_{0.5}$ is the V_m for 50% charge movement, F is Faraday's constant, R is the gas constant, and T is the absolute temperature.

Three different protocols were used to extract the carrier-mediated current transients from the total current traces. (*i*) Transients were obtained by fitting the total current traces in the presence of 100 mM NaCl (in the absence of GABA) to Equation 2 as described above. (*ii*) Transients were obtained by direct subtraction of the current traces obtained in the presence (100 mM) and absence of external Na^+. (*iii*) Transients were obtained by direct subtraction of current traces in the absence and presence (1 mM) of GABA (*see* below for details).

The latter two protocols require that the current trace that contains no transporter charge movement (I_o; e.g., in the absence of external Na^+, or in the presence of saturating GABA) be subtracted from the one that contains maximum charge (I_q; e.g., in the presence of 100 mM NaCl, and in the absence of GABA). To

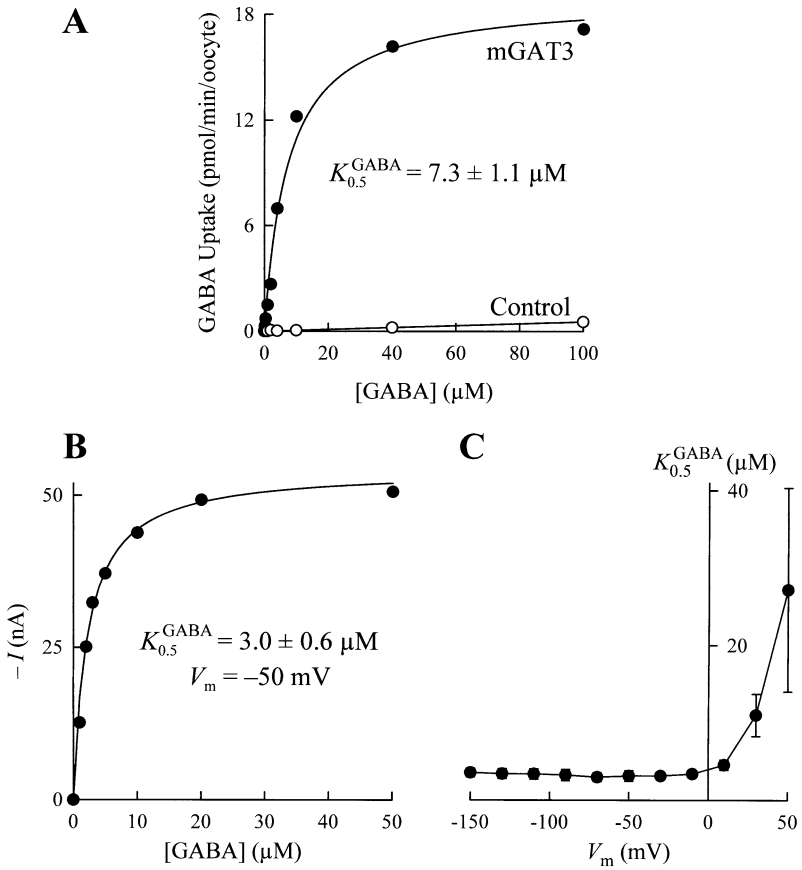

Fig. 2. Kinetics of GABA transport. (*A*) GABA uptake into nonvoltage-clamped mGAT3-expressing oocytes was saturable with a $K_{0.5}^{GABA}$ of 7.3 ± 1.1 μM ($N \geq 10$ oocytes at each GABA concentration) (*filled circles*). The Smooth line is the fit of the data to Equation 1. GABA uptake into control oocytes was minimal ($N \geq 10$) (*open circles*). The smooth line represents a linear regression through the data points. (*B*) The GABA-evoked inward current in mGAT3-expressing cells was also saturable with a $K_{0.5}^{GABA}$ of 3.0 ± 0.6 μM (V_m = −50 mV) (N = 6). (*C*) At negative membrane potentials, $K_{0.5}^{GABA}$ was relatively voltage-independent (≈3 μM), but increased at positive membrane potentials.

correct for background as well as GABA-evoked steady-state inward currents, before and after the voltage pulse, the subtracted current trace ($I_{Subtracted}$) was obtained by:

$$I_{Subtracted}(t) = [I_q(t) - I_q^{Holding}] - [I_o(t) - I_o^{Holding}] \quad (4)$$

and during the voltage pulse, $I_{Subtracted}$ was obtained by:

$$I_{Subtracted}(t) = [I_q(t) - I_q^{Steady-State}] - [I_o(t) - I_o^{Steady-State}] \quad (5)$$

where $I^{Holding}$ is the holding current and $I^{Steady\text{-}State}$ is the steady-state current at the end of the voltage pulse. The integral of the subtracted trace yielded the charge, and the fit of the Q-V relationship to the Boltzmann function (Equation 3) yielded the Q_{max}.

Presteady-state and steady-state curve fittings were performed by using either SigmaPlot (SPSS Science; Chicago, IL), or software developed in this laboratory (using a Marquardt-Levenberg algorithm). Where sample sizes are indicated (N), they refer to the number of oocytes in which the experiments were repeated. Reported errors represent the standard error of the mean obtained from data from several oocytes.

Results

Steady-State Characteristics of mGAT3 GABA Transport

In the presence of Na^+ (100 mM) and Cl^- (106 mM) in the bathing medium of voltage-clamped (−50 mV) mGAT3-expressing oocytes, addition of GABA to the bath caused an inward current (Fig. 1*A*). Correspondingly, under nonvoltage-clamp conditions, GABA induced a membrane depolarization (*not shown*). The magnitude of both GABA-evoked membrane depolarization and inward current depended on the level of mGAT3 expression in the plasma membrane (*see* Fig. 12). The GABA-evoked current was absolutely dependent on external Na^+, but in the absence of external Cl^-, ≈50% of the activity was retained (Fig. 1*A*). The specific inhibitor of GAT-1, SKF 89766-A, had no inhibitory effect on the mGAT3 GABA-induced inward current (*not shown*).

The GABA-evoked current was examined as a function of the membrane voltage (V_m). In the voltage range −150 mV to +50 mV, the current-voltage (I-V) relationship was fairly linear (Fig. 1*B*). The GABA-induced net inward charge (i.e., integral of the inward current) was directly proportional to GABA uptake into cells (2.2 ± 0.1 charges/GABA) (Fig. 1*C*) and, therefore, may be used as an assay of mGAT3 transport rate.

Both GABA uptake and the inward current induced by GABA were saturable and followed hyperbolic kinetics (Fig. 2*A* and *B*). The half-maximal concentration for GABA ($K_{0.5}^{GABA}$) uptake was 7.3 ± 1.1 μM ($N \geq 10$ oocytes at each GABA concentration), and that for the GABA-induced inward current

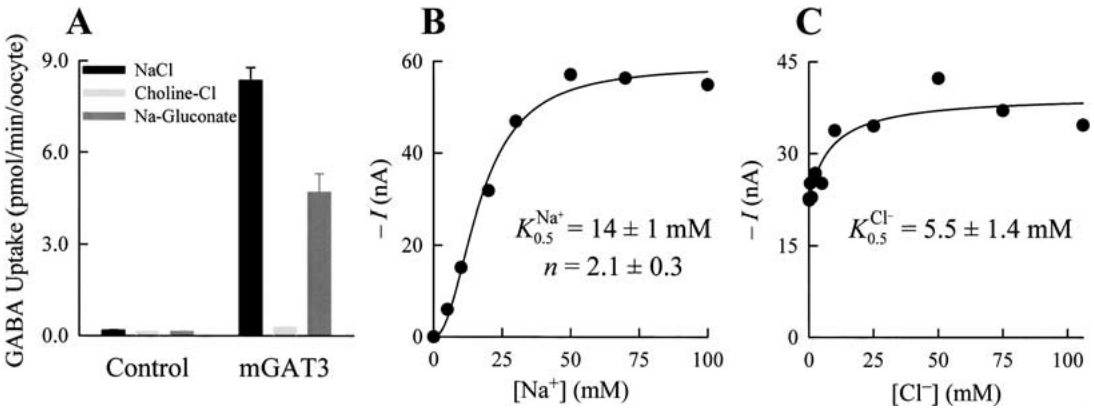

Fig. 3. Na^+- and Cl^--dependence of mGAT3 GABA transport. (*A*) GABA uptake into mGAT3-expressing oocytes was strictly dependent on external Na^+, however, external Cl^- was not absolutely required (*see* also Fig. 1*A*). The data for each bar represent mean ± SE from at least 10 control and 15 mGAT3-expressing cells. Similar results have been obtained with cells from four donor frogs. (*B*) Similar to GABA uptake, the GABA-induced inward current was strictly dependent on external Na^+ (V_m = −50 mV). The Na^+-dependence of the GABA-evoked (500 μM, 106 mM $[Cl^-]_o$) current followed a sigmoidal relationship with a Hill coefficient of 2.1 ± 0.3 (N = 4). The half-maximal Na^+ concentration ($K_{0.5}^{Na^+}$) was 14 ± 1 mM (N = 4). The smooth line is the fit of the data to Equation 1. (*C*) In the absence of external Cl^-, the current was reduced by ≈50% (V_m = −50 mV). Cl^- enhancement of the GABA-evoked (500 μM, 100 mM $[Na^+]_o$) current followed hyperbolic kinetics. The Cl^- concentration ($K_{0.5}^{Cl^-}$) required for half-maximal enhancement of the GABA-evoked current was 5.5 ± 1.4 mM (N = 3). The Hill coefficient for Cl^- enhancement was ≈1. The smooth line is the fit of the data to Equation 1, in which an additional linear term was added to account for the non-zero baseline at zero Cl^- concentration.

was 3.0 ± 0.6 μM (V_m = −50 mV) (N = 6). The Hill coefficient for GABA activation of the inward currents was 1.1 ± 0.1 (N = 6). $K_{0.5}^{GABA}$ was relatively voltage-independent at negative voltages, and only at positive membrane potentials (≥30 mV) did its value rise significantly (Fig. 2*C*). GABA uptake into oocytes was uphill, as after 30-min incubation periods in 100 μM GABA, the intracellular GABA concentration was estimated to be ≥1 mM (assuming a cytoplasmic volume of 500 nl), a greater than 10-fold accumulation (e.g., based on Fig. 2*A*). Maximum accumulating capacity is much higher, as at 30 minutes, the transport rate still represents the initial rates. Five-hour incubation periods under identical conditions lead to >50-fold concentration of GABA into oocytes (*not shown*). Therefore, mGAT3 can accumulate GABA against a concentration gradient.

Na^+ and Cl^- Dependence of mGAT3 GABA Transport

mGAT3 GABA transport was strictly Na^+ dependent (Fig. 1*A* and Fig. 3*A* and *B*). In the absence of Na^+ in the bath (106 mM Cl^- present), GABA influx was reduced to that seen in control cells (Fig. 3*A*). The Cl^--dependence was not absolute, as removal of Cl^- (at 100 mM Na^+) reduced GABA influx by only ≈45%. GABA uptake in the absence of external Cl^- was 56 ± 7% of that in the presence of 106 mM $[Cl^-]_o$ (N = 15 cells from three batches; Fig. 3*A*). In agreement with the uptake experiments, in the absence of external Na^+ (106 mM Cl^-), no GABA-evoked inward current was observed (Figs. 1*A* and 3*B*), whereas in the absence of external Cl^- (100 mM Na^+), the GABA-evoked current was ≈55% of that induced in the presence of 106 mM Cl^- (57 ± 4%; N = 8)(Figs. 1*A* and 3*C*).

At a membrane potential of −50 mV (at 106 mM $[Cl^-]_o$ and 0.5 mM GABA), the mGAT3 half-maximal concentration for Na^+ ($K_{0.5}^{Na^+}$) was 14 ± 1 mM (N = 4) (Fig. 3*B*). The Hill coefficient for Na^+ activation of the inward currents was 2.1 ± 0.3 (N = 4). At 100 mM $[Na^+]_o$ and 0.5 mM GABA, increasing the $[Cl^-]_o$ led to an enhancement of the GABA-evoked current in a concentration-dependent manner. The $[Cl^-]_o$ ($K_{0.5}^{Cl^-}$) needed to achieve half-maximal enhancement of the GABA-evoked inward current was 5.5 ± 1.4 mM (N = 3) (Fig. 3*C*). The Hill coefficient for the Cl^--enhancement of the GABA-evoked inward current was 1.1 ± 0.1 (N = 3).

Presteady-State Current Transients (Charge Movements) of mGAT3

In the absence of GABA and in the presence of NaCl, voltage pulses induced mGAT3-mediated presteady-state current transients (Fig. 4*A*). The presteady-state transients may be isolated from the capacitive and steady-state components by point-by-point subtraction of the records in the presence and absence of external Na^+ (Fig. 4*B*) (*see* Materials and Methods) (Hazama, Loo & Wright, 1997; Mager et al., 1993). At each test voltage, the integral of the current transients for the ON response (in Fig. 4*B*) yielded the charge-voltage (Q_{ON}-V) relation (Fig. 4*C*). The voltage for half-maximal translocation of

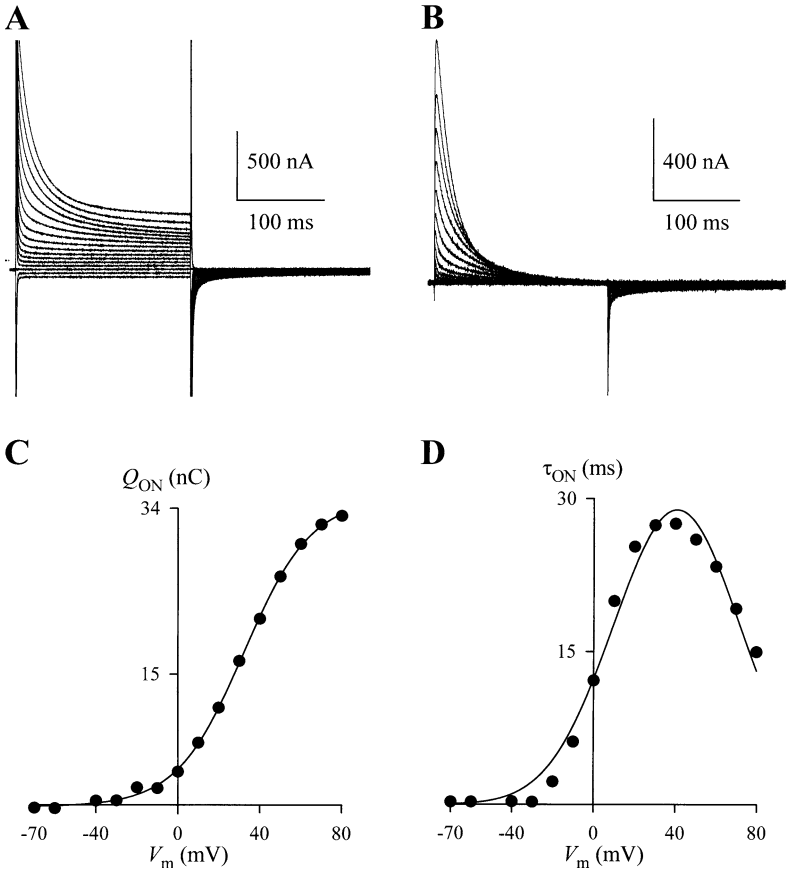

Fig. 4. Presteady-state charge movements of mGAT3. (*A*) In response to step changes in the membrane potential, mGAT3 exhibited current transients. The transients were preceded by oocyte plasma membrane capacitive currents ($\tau \approx 0.5$ msec), which are present in control cells as well. The mGAT3 transients were most pronounced for the ON response. The OFF transients relaxed slowly to a steady state (*see* text and Figs. 5 and 6). The holding potential was −50 mV, and the voltage pulses (200 msec) ranged from +80 mV to −70 mV in 10-mV steps. The dashed line represents the zero current level. Control oocytes do not exhibit presteady-state transients (*not shown*). (*B*) Presteady-state charge movements were obtained after subtraction of the records in the absence of Na^+ (choline-Cl replacement; *see* Fig. 7). This manipulation removes the oocyte capacitive currents, as well as the steady-state oocyte leak currents (*see* Materials and Methods). (*C*) At each applied voltage, time integration of the ON transients in panel *B* yielded the charge moved. The charge-voltage (*Q-V*) relationship obtained was fitted to a single Boltzmann function (Equation 3). For the records shown, the Boltzmann parameters obtained from the fit were: Q_{max}, 35 nC; $V_{0.5}$, 32 mV; $z\delta$, 1.6. (*D*) The mGAT3 ON transients relaxed exponentially to zero. The time constant of the relaxation (τ_{ON}) as a function of the test voltage (τ_{ON}-*V* relationship) followed a bell-shaped function. The voltage at maximum τ_{ON} was 36 mV. This voltage is similar to the $V_{0.5}$ of the *Q-V* relationship (panel *C*). The smooth line is the fit of the data to a bell-shaped function of the form $\tau = \tau_{max} \exp\left[-0.5\left(\frac{V_m - V_{\tau max}}{s}\right)^2\right]$, where τ is the time constant, τ_{max} is the maximum value of τ, V_m is the membrane voltage, $V_{\tau max}$ is the V_m at which τ_{max} occurs, and s is a measure of the spread of the distribution.

the charge ($V_{0.5}$) was 29 ± 1 mV ($N = 35$), and the effective valence of the moveable charge ($z\delta$) was 1.6 ± 0.1 ($N = 35$). Q_{max} depended on the level of mGAT3 expression in the plasma membrane (*see* Fig. 12). The relaxation of the ON transients was adequately described by a single exponential function. The decay time constant plotted as a function of the test voltage (τ_{ON}-*V* relation) followed a bell-shaped function with a maximum value of 32 ± 2 msec ($N = 35$) (Fig. 4*D*). The voltage at maximum τ_{ON} (33 ± 2 mV; $N = 35$) was similar to the $V_{0.5}$ of the *Q-V* curve (Fig. 4*C*).

mGAT3 Q_{ON} and Q_{OFF} are Equal

In contrast to the ON response, the OFF transients decayed very slowly to a steady-state. Consequently, for the 200-msec voltage pulses shown in Fig. 4*A* and *B*, the OFF transients appeared to be considerably smaller in magnitude than the ON transients. However, when the OFF transients were recorded for long periods (≥3 sec) until they fully decayed to a steady state (Fig. 5*A*), Q_{ON} and Q_{OFF} were equal in magnitude (Fig. 5*B*). To examine the time course for charge recovery, we applied two depolarizing pulses in succession, and varied the interval between the two pulses (Fig. 6*A*). For each pulse, the charge moved (Q_{ON}) was determined (Fig. 6*B*). The recovery of charge (i.e., the magnitude of *Q* for the second pulse) was critically dependent on the inter-pulse interval; Q_{ON} for the second pulse decreased exponentially as the interval between the two pulses was shortened (Fig. 6*C*). The time constant for the recovery of charge ($\tau_{Recovery}$) was 1.1 ± 0.1 sec ($N = 5$).

Because of the slow relaxation of the OFF transients, the following discussion of the presteady-state currents will involve those examined for the ON response to voltage perturbations. The voltage pulses used ranged from 200–400 msec, but no significant differences were observed in the ON responses when longer pulses (up to 800 msec) were applied (*not shown*).

Determination of Q_{max}

Since Q_{max} is a good indicator of the level of transporter expression in the plasma membrane (Loo et al., 1993; Wadiche et al., 1995; Zampighi et al., 1995; Hirsch, Loo & Wright, 1996; Mager et al., 1996; Eskandari et al., 2000), we wished to establish the

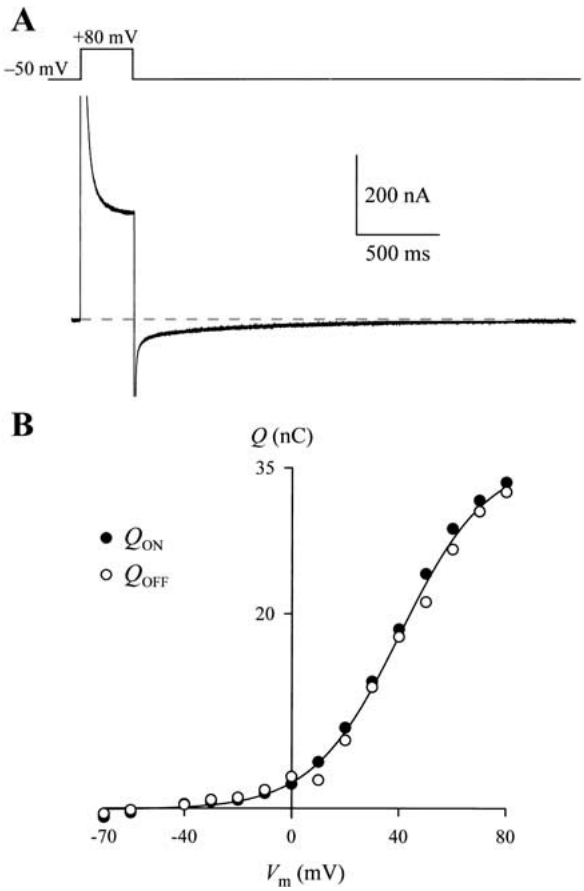

Fig. 5. Q_{ON} and Q_{OFF} are equal in magnitude. (*A*) Shown is the current trace in response to a 320-msec pulse (−50 mV to +80 mV). The OFF transient was recorded for 3 sec until the presteady-state currents decayed back to the holding current (*dashed line*). Notice that the OFF transient takes >3 seconds to reach steady state. (*B*) Q_{ON} (*filled circles*) and Q_{OFF} (*open circles*) were determined from a series of voltage pulses ranging from +80 mV to −70 mV in 10-mV steps (−50 mV holding voltage). The duration of the pulses was as shown in panel *A*. The smooth line represents a Boltzmann fit (Equation 3) to the average of Q_{ON} and Q_{OFF}.

optimal conditions under which Q_{max} can be measured. Three different protocols were used to obtain Q_{max} (*see* Materials and Methods for details). (*i*) Q_{max} was determined from the carrier-mediated transients obtained by fitting the total current traces in the presence of 100 mM NaCl (in the absence of GABA) to Equation 2. (*ii*) Q_{max} was determined from the carrier-mediated transients obtained by direct subtraction of the current traces in the presence (100 mM) and nominal absence of external Na^+. (*iii*) Q_{max} was determined from the carrier-mediated transients obtained by direct subtraction of current traces in the absence and presence (1 mM) of GABA. When tested in the same cells, all three protocols yielded similar Q_{max} values (Fig. 7). Therefore, the presteady-state charge movements depend entirely on external Na^+ and are completely eliminated in the presence of saturating GABA concentrations.

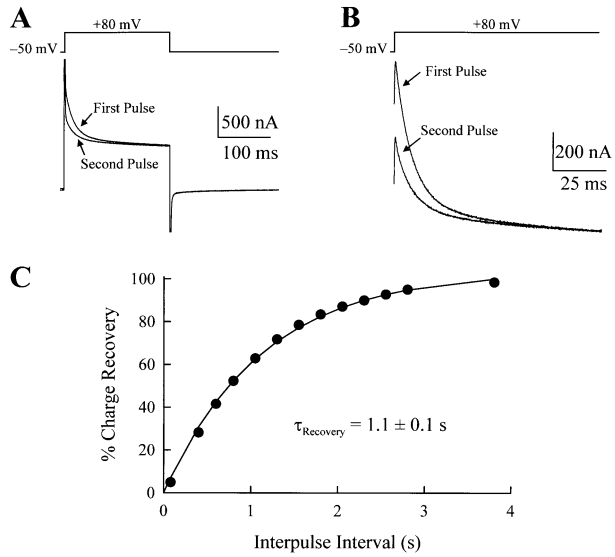

Fig 6. Slow relaxation of Q_{OFF}. (*A*) Two pulses (200 msec) were applied in succession with a defined inter-pulse interval. The traces represent two voltage pulses from the holding potential of −50 mV to +80 mV. The first pulse was followed by the second pulse after an interval of 200 msec. Notice that when the second pulse was applied, the OFF transients had not yet decayed to a steady state. (*B*) The presteady-state charge movements were extracted from the total current traces in panel *A* (via curve fitting). The charge moved in response to the first pulse was 18.4 nC, whereas that in response to the second pulse was 10.8 nC. (*C*) Two pulses were applied in succession (as in panel *A*) while the interpulse interval was varied. The charge moved in response to the second pulse was expressed as a percentage of the charge moved in response to the first pulse (% Charge Recovery). Percent charge recovery was then plotted as function of the interpulse interval. The data can be described by a single rising exponential function with a time constant ($\tau_{recovery}$) of 1.1 ± 0.1 sec (N = 5).

Charge Movements Exhibit a Fast and a Slow Phase

The subtraction method was used in the presence and absence of external Na^+ to isolate the transporter-mediated charge movements (*see* Fig. 7). The subtracted traces revealed a rapid rising phase of the charge movements followed by slower mono-exponential decay to the steady-state (Fig. 8*A*). The time-to-peak for the rapid phase was ≤2 msec, and appeared to be slightly voltage dependent (*inset* in Fig. 8*A*). Correspondingly, the time integral of the ON transients of Fig. 8*A* could be well fitted with a rising two-exponential function, with time constants of ≤2 msec and ≤30 msec (Fig. 8*B*).

Presteady-State Charge Movements in the Presence of GABA

In the presence of saturating concentrations of GABA, no presteady-state currents were observed, as Q_{max} was below the resolution of the measurements (≈2 nC) (Figs. 7, 9*A*, and *B*). The reduction in charge

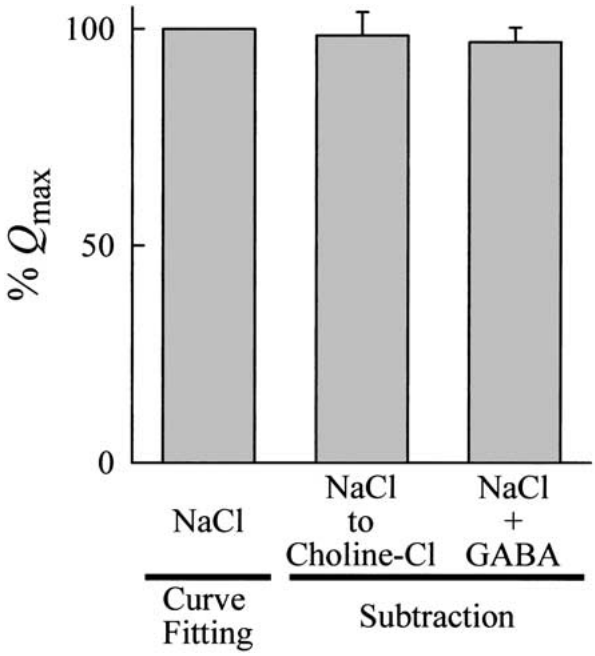

Fig. 7. Three valid methods of Q_{max} determination. Bar graph showing the results of Q_{max} determination from (*i*) curve fitting of the total current traces, (*ii*) subtraction of current traces in replacing NaCl in the bath with choline-Cl, and (*iii*) subtraction of the current traces in going from NaCl in the bath to NaCl plus saturating GABA (1 mM) (*see* text for details). Voltage pulses ranged from +80 mV to −70 mV in 10-mV steps. All Q_{max} determinations were normalized to Q_{max} determined in the same cell via the curve-fitting method. Data represent the mean ± SE from at least five oocytes. In the voltage range tested, the charge movements are absolutely dependent on external Na^+ and, in addition, are fully abolished when the transporter achieves maximum transport rates in the presence of saturating concentrations of substrate.

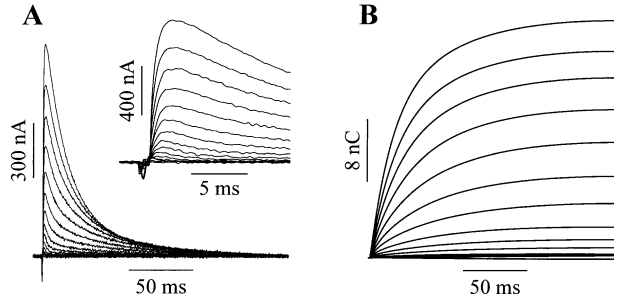

Fig. 8. Relaxation of the ON charge movements. (*A*) Current transients were obtained in the presence and absence of external Na^+ (NaCl to choline-Cl; voltage pulses ranged from +80 mV to −70 mV in 10-mV steps), and the presteady-state charge movements were extracted for the ON response via the subtraction method. *Inset* shows the first 15 msec after the onset of the voltage pulses. There was a rapid rising phase (time to peak ≤ 2 msec) followed by a slower decay ($\tau \leq 30$ msec) to the steady state. The OFF transients are not shown. (*B*) Time integral of the presteady-state current transients of panel *A*. The data can be fitted to a two-exponential function, with time constants of ≤ 2 msec and ≤ 30 msec.

was dependent on the GABA concentration (Fig. 9*C* and *D*); as the GABA concentration was increased, Q_{max} decreased in a hyperbolic fashion (Fig. 9*E*). The GABA concentration for 50% reduction in Q_{max} (K_i^{GABA}) was 5.1 ± 0.3 μM ($N = 3$), $V_{0.5}$,$z\delta$ (Fig, 9*D*), and the relaxation time constants were not significantly altered by GABA (*not shown*).

Na^+ Dependence of the Presteady-State Charge Movements

Reduction in $[Na^+]_o$ led to a decrease in Q_{max}, as well as a shift in the *Q-V* relationship toward negative membrane potentials (Fig. 10*A–D*). The shift in $V_{0.5}$ was ≈ −100 mV for a 10-fold reduction in $[Na^+]_o$. As $[Na^+]_o$ was increased from 100 mM to 150 mM, $V_{0.5}$ shifted from ≈35 mV to ≥75 mV, and a reliable fit of the *Q-V* curve was not possible (*not shown*). At nominal zero $[Na^+]_o$ (106 mM Cl^- present), Q_{max} was below the resolution of the measurements (≈2 nC). The increase in Q_{max} as a function of $[Na^+]_o$ followed a sigmoidal relationship with a half-maximal concentration of 48 ± 3 mM, and a Hill coefficient of 2.4 ± 0.2 ($N = 6$) (Fig. 10*E*). As $[Na^+]_o$ was reduced (*i*) the maximum value of τ_{ON} decreased from 30 msec at 100 mM Na^+ (at $V_m \approx 30$ mV) to 10 msec at 20 mM Na^+ (at $V_m \approx -50$ mV); (*ii*) at each $[Na^+]_o$ the voltage at maximum τ_{ON} was similar to the $V_{0.5}$ of the Q_{ON}-*V* relationship; and (*iii*) there was no significant change in the apparent valence of the moveable charge ($z\delta$) (*not shown*).

Cl^- Dependence of the Presteady-State Charge Movements

As the steady-state characteristics were dependent on $[Cl^-]_o$ (*see* Figs. 1*A*, 3*A*, and *C*), we examined the Cl^--dependence of the voltage-induced presteady-state charge movements (Fig. 11*A* and *B*). Similar to the reduction in $[Na^+]_o$, the *Q-V* relationship was shifted to negative potentials as $[Cl^-]_o$ was reduced from 106 mM to 0 mM (Fig. 11*C*); $V_{0.5}$ shifted from ≈40 mV to ≈ −5 mV. Unlike the strict dependence on Na^+, in the absence of external Cl^- (100 mM Na^+ present), significant presteady-state charge movements were observed (compare panels *A* and *B* in Fig. 11). At nominal zero $[Cl^-]_o$, Q_{max} was 30 ± 5% of Q_{max} at 106 mM Cl^- ($N = 4$) (Fig. 11*D*). Cl^- enhancement of charge movements was saturable with a half-maximal concentration of 19 ± 3 mM ($N = 4$). As the Cl^- concentration was reduced, the relaxation time constants became slightly smaller; at its maximum value, τ_{ON} decreased from 30 msec (at 106 mM Cl^- and ≈40 mV) to 20 msec at nominal zero $[Cl^-]_o$ (at ≈ −5 mV) (*not shown*). Variations in $[Cl^-]_o$ did not alter the apparent valence of the moveable charge ($z\delta$; *not shown*).

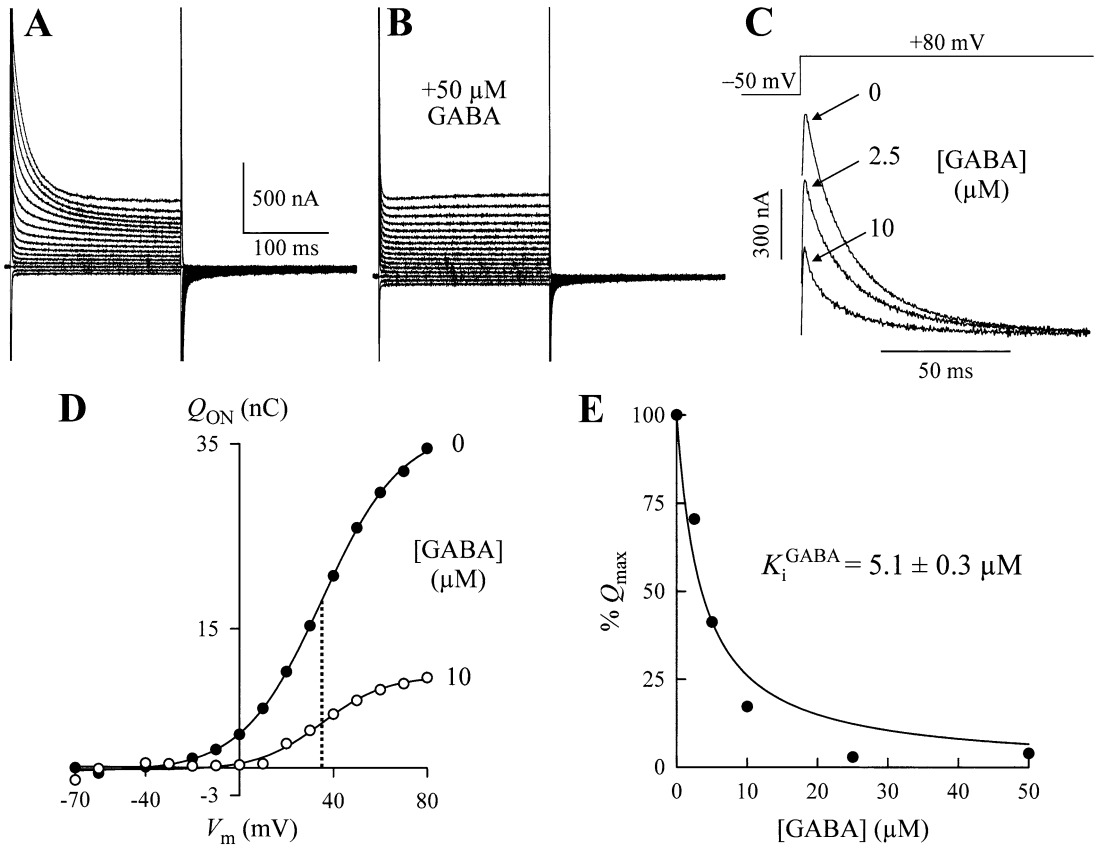

Fig. 9. Diminution of charge movements in the presence of GABA. (*A*) Raw current traces obtained in response to 200-msec voltage pulses ranging from +80 mV to −70 mV in 10-mV steps ($[Na^+]_o$ = 100 mM and $[Cl^-_o$ = 106 mM). (*B*) Current records obtained in the presence of 50 μM GAB A from the same cell as that in panel *A*. Notice the near complete abolition of the presteady-state currents. (*C*) The presteady-state charge movements were isolated via the curve-fitting method and are shown (−50 to +80 mV voltage step) in the absence (0 GABA) and presence of 2.5 and 10 μM GABA. (*D*) Q_{ON}-V curves in the absence (*filled circles*) and presence of 10 μM GABA (*open circles*). Despite the reduction in Q_{max}, the voltage for half-maximal translocation of the charge ($V_{0.5}$ = 35 mV; *dotted line*) was not altered by GABA. Neither the voltage distribution (τ_{ON}-V) nor the absolute values of the relaxation time constants were altered by GABA (*not shown*). (*E*) The GABA-induced reduction in Q_{max} was concentration dependent; 50% reduction occurred at 5.1 ± 0.3 μM (K_i^{GABA}) (N = 3). Saturating GABA concentrations led to the complete abolition of the presteady-state charge movements (*see* also Fig. 7).

mGAT3 Steady-State Turnover Rate

The turnover rate (*TO*) of the transporter can be estimated according to $I_{max} = Q_{max} \cdot TO$ (Mager et al., 1993; Mackenzie et al., 1996; Eskandari et al., 1997). In a group of oocytes, both Q_{max} and I_{max} were measured. In each oocyte, Q_{max} was measured and, subsequently, I_{max} was measured at 1 mM GABA. The slope of the plot I_{max} *vs.* Q_{max} provided an estimate of the turnover rate of mGAT3 (Fig. 12). The mGAT3 turnover rate was 1.7 ± 0.1 sec^{-1} at −50 mV (N = 34), and 3.8 ± 0.2 sec^{-1} at −150 mV (N = 21).

Discussion

Despite widespread distribution of the four mammalian GABA transporter isoforms in the central nervous system (GAT1–GAT4) as well as in the periphery (GAT2 and GAT3), the functional characteristics of GAT3 and GAT4 have received little attention. It is well established that the isoforms exhibit substantial differences with respect to the primary sequence, substrate selectivity and pharmacology and, moreover, it is evident that the isoforms differ in their localization within the central nervous system (Borden, 1996; Lill & Nelson, 1998; Nelson, 1998; Jursky & Nelson, 1999; Gadea & López-Colomé, 2001). In view of the potential use of the GABA transporters as therapeutic targets for the treatment of epileptic seizures (Roettger & Amara, 1999; Schachter, 1999) as well as stroke (Green, Hainsworth & Jackson, 2000), it is necessary that the function of all isoforms be thoroughly understood. Moreover, individual isoforms may exhibit unique features that lead to a better understanding of the mechanism of Na^+/Cl^-/GABA cotransport. In an

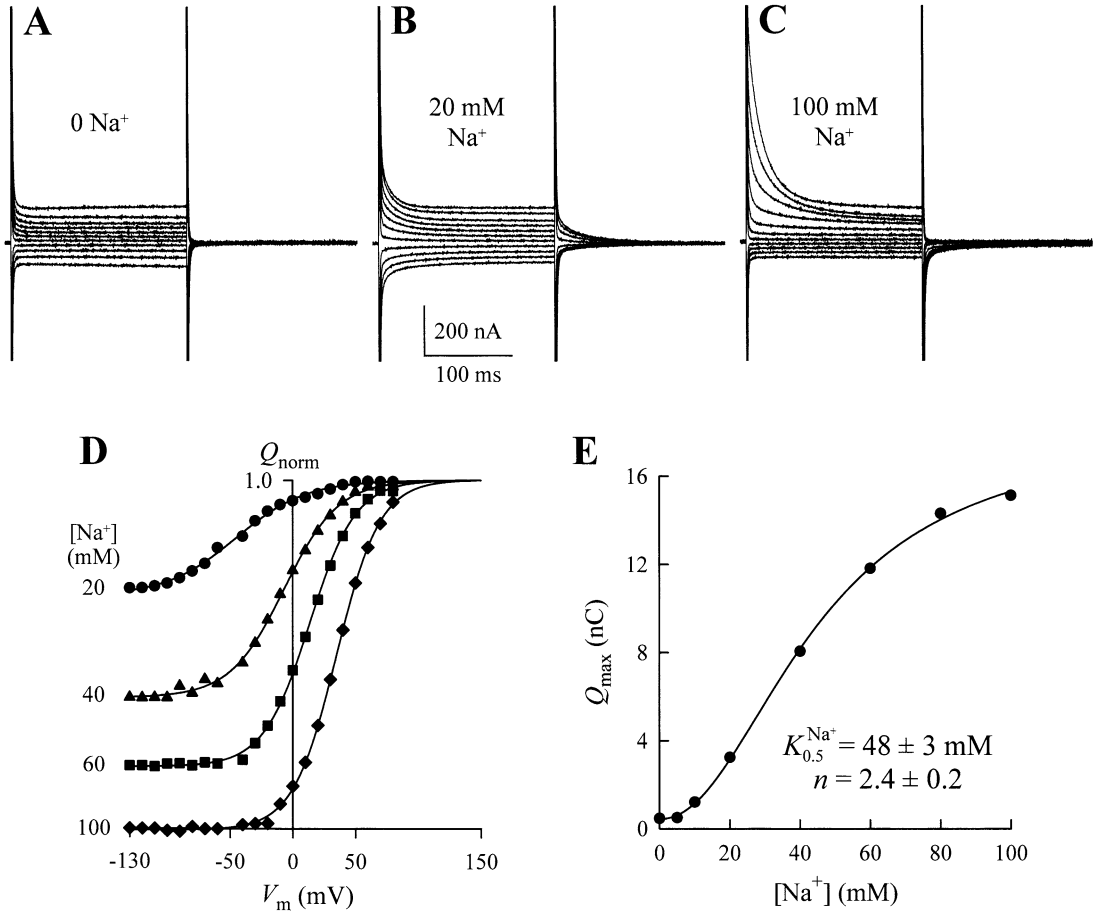

Fig. 10. Na^+ dependence of the presteady-state charge movements. (*A*) Raw current traces were obtained in response to 200-msec voltage pulses ranging from +80 mV to −130 mV in 10-mV steps. The holding voltage was −50 mV. These records were obtained in the absence of external Na^+ ($[Cl^-]_o$ = 106 mM). Notice the absence of presteady-state currents. (*B* and *C*) Current records were obtained in the presence of 20 mM and 100 mM Na^+ ($[Cl^-]_o$ = 106 mM). Notice the appearance of presteady-state currents, and also the difference in the distribution of the charge movements with respect to the applied voltage. Records in panels *A–C* were obtained from the same cell. For clarity, only 11 of the 22 traces recorded are shown. (*D*) Charge-voltage (*Q-V*) relationships at various $[Na^+]_o$. As the $[Na^+]_o$ was reduced ($[Cl^-]_o$ = 106 mM), there was a reduction in Q_{max}, and the *Q-V* curves shifted to the left. $V_{0.5}$ shifted ≈ −100 mV for a 10-fold reduction in $[Na^+]_o$. For comparison, the *Q-V* curves have been normalized with respect to Q_{dep} at 100 mM $[Na^+]_o$ and shifted vertically such that all Q_{dep} values are aligned with Q_{dep} at 100 mM Na^+ (*see* Loo et al., 1993; Mager et al., 1993). (*E*) In the absence of external $[Na^+]_o$, no presteady-state charge movements were observed. There was a sigmoidal dependence of Q_{max} on $[Na^+]_o$ ($[Cl^-]_o$ = 106 mM). The half-maximal concentration was 48 ± 3 mM, and the Hill coefficient was 2.4 ± 0.2 (N = 4).

effort to augment our understanding of the GABA transporters, here we present electrophysiological and tracer uptake data for a functional characterization of mouse GAT3.

Steady-State Transport Characteristics

Like other members of the Na^+- and Cl^--dependent family of neurotransmitter transporters, mGAT3 was found to be electrogenic (Kavanaugh et al., 1992; Mager et al., 1993, 1996; Galli et al., 1995; Sonders et al., 1997; Matskevitch et al., 1999; Cao, Mager & Lester, 1998; Loo et al., 2000). The electrogenicity of transport suggests that net positive charge enters the cell as a result of transporter activity. The coupling ratio between the net inward charge and GABA influx (2.2 ± 0.1 charges/GABA) is similar to that determined for human GAT1 (Loo et al., 2000), but different from that reported for GAT2/BGT-1 (1 charge/GABA) (Matskevitch et al., 1999). The stoichiometry for GAT1 is 2 Na^+: 1 Cl^-: 1 GABA (Loo et al., 2000), and that for GAT2/BGT-1 has been proposed to be 3 Na^+: 2 Cl^-: 1 GABA or 3 Na^+: 1 Cl^-: 1 GABA (Matskevitch et al., 1999). The Hill coefficient of 2 for Na^+ activation of steady-state currents (Fig. 3*B*), and the hyperbolic nature of Cl^- enhancement of the steady-state currents (Fig. 3*C*) suggest that 2 Na^+ and 1 Cl^- may be involved in the transport cycle of mGAT3. In addition, the electrogenicity of transport suggests that the transport cycle

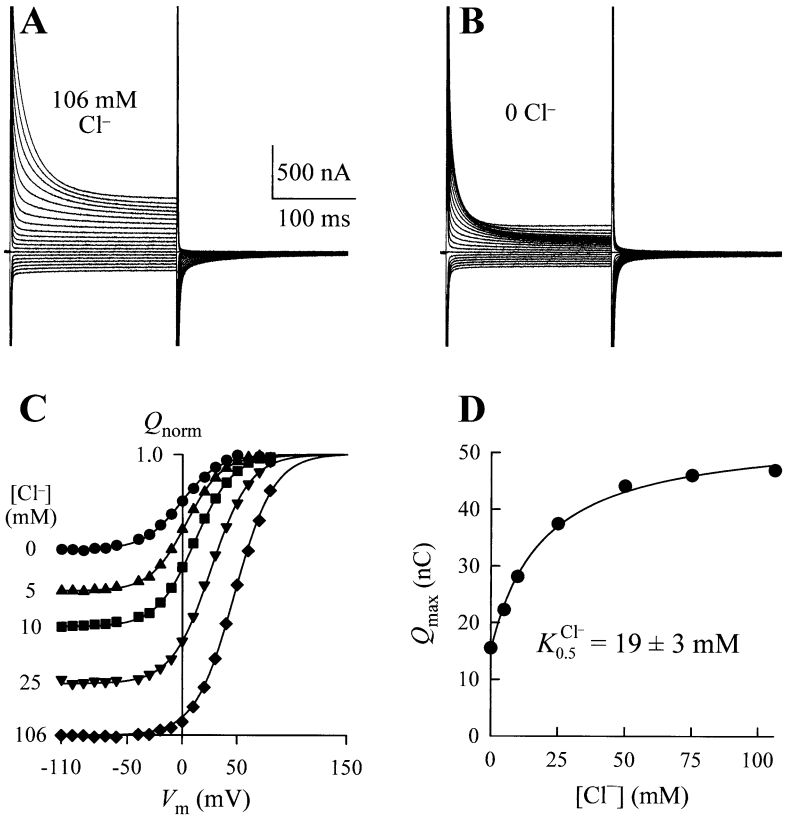

Fig. 11. Cl^--dependence of the presteady-state charge movements. (*A*) Current traces were obtained in response to a series of 200-msec voltage pulses ranging from +80 mV to −110 mV in 10-mV steps. The holding voltage was −50 mV. These records were obtained in the presence of 100 mM external Na^+, and 106 mM external Cl^-. (*B*) Current traces were obtained in the nominal absence of external Cl^- ($[Na^+]_o = 100$ mM). Note the reduction in the presteady-state transients in the absence of external Cl^-. Also note the change in the distribution of the charge movements with respect to the applied voltage. The pulse protocol was like that in panel *A*. (*C*) Charge-voltage (*Q-V*) relations at various $[Cl^-]_o$ ($[Na^+]_o = 100$ mM). As $[Cl^-]_o$ was reduced, there was a reduction in Q_{max}, and the midpoint ($V_{0.5}$) of the *Q-V* curve shifted toward negative potentials; $V_{0.5}$ shifted from ≈40 mV at 106 mM $[Cl^-]_o$ to ≈ −5 mV at nominal zero $[Cl^-]_o$. The *Q-V* curves have been normalized with respect to Q_{dep} at 106 mM Cl^- (*see* legend to Fig. 10). The τ_{ON}-*V* relations at various $[Cl^-]_o$ were shifted to the left such that the voltage at peak τ_{ON} was similar to the corresponding $V_{0.5}$ (*not shown*). The maximum value of τ_{ON} was reduced from 30 msec at 106 mM Cl^- to 20 msec at zero $[Cl^-]_o$ (*not shown*). $z\delta$ (1.5; obtained from the Boltzmann fit) was not altered by variations in $[Cl^-]_o$ (*not shown*). (*D*) Q_{max} as a function of $[Cl^-]_o$ ($[Na^+]_o = 100$ mM). At nominal zero $[Cl^-]_o$, Q_{max} was 30 ± 5% of that at 106 mM $[Cl^-]_o$. The Cl^--induced increase in Q_{max} was concentration dependent with a half-maximal concentration of 19 ± 3 mM ($N = 4$).

may be sensitive to the imposed potential difference across the membrane. Indeed, transport rates approached zero at positive membrane potentials and increased in a near-linear fashion at hyperpolarizing membrane potentials. The near-linear steady-state *I-V* relationship suggests that in the voltage range tested, the rate-limiting step in the transport cycle is a voltage-dependent step (Läuger, 1991).

GABA transport is energized by Na^+. Although Cl^- can significantly enhance the rate of transport, it is not absolutely essential. In the absence of Na^+, Cl^- cannot drive transport or, alternatively, Na^+-independent Cl^--driven GABA transport rate is below the detection limit (*not shown*). Therefore, the role of Cl^- may be one of facilitation (Loo et al., 2000). It is now well documented that the dependence of GABA transporters on external Cl^- is not absolute (Borden et al., 1992; Kavanaugh et al., 1992; Keynan et al., 1992; Mager et al., 1993; Clark & Amara, 1994; Lu & Hilgemann, 1999a; Matskevitch et al., 1999; Loo et al., 2000). As transport rates appear to be strongly regulated by both extracellular and cytoplasmic Cl^- concentrations (Loo et al., 2000; Lu & Hilgemann, 1999a,b; Mager et al., 1993), it is of particular interest to document the exact role of Cl^- in the transport cycle. For GAT1, it has been suggested that Cl^- is thermodynamically coupled to Na^+/GABA cotransport (Lu & Hilgemann, 1999a; Pastuszko, Wilson & Erecinska, 1982), however, recent data are also suggestive of a strong kinetic role for Cl^- with no net transport of Cl^- during the transport cycle (Loo et al., 2000). Future experiments will be needed in order to better understand the role of Cl^- in these transporters. Interestingly, mGAT3 exhibits a significantly higher affinity for Cl^- than does GAT1. Such differences have also been reported for isoforms of the related glycine transporter (López-Corcuera et al., 1998), and may provide clues about physiological and/or pathophysiological regulation of these transport proteins.

The half-maximal concentration for GABA ($K_{0.5}^{GABA}$) is relatively voltage independent for a wide range of membrane potentials, and only becomes voltage dependent at the more positive potentials (Fig. 2*B*). This property may have important physiological significance in that despite neuronal and/or glial electrical activity, mGAT3 maintains its ability to transport GABA. Nonetheless, the transporter turnover rate is highly voltage dependent, becoming smaller at more depolarized membrane potentials.

Some neurotransmitter transporters have been shown to exhibit substrate-evoked currents in excess

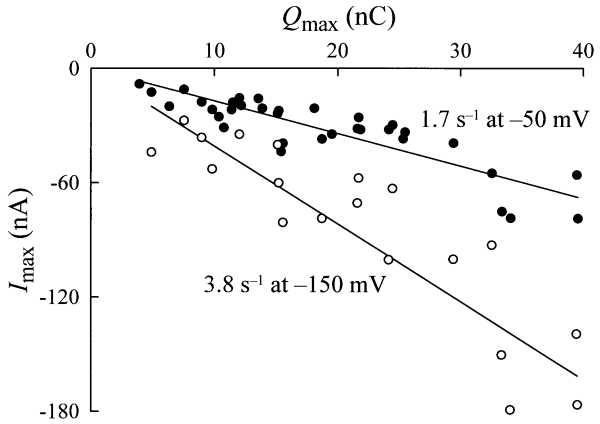

Fig. 12. mGAT3 steady-state turnover rate. In a group of mGAT3-expressing cells, both Q_{max} (by curve fitting in the absence of GABA) and I_{max} (at 1 mM GABA) were measured, $I_{max} = Q_{max} \cdot TO$, where TO is the turnover rate. At −50 mV, the mGAT3 turnover rate was 1.7 ± 0.1 sec^{-1} (*filled circles*; $N = 34$). At −150 mV, the turnover rate was 3.8 ± 0.2 sec^{-1} (*open circles*; $N = 21$). Each data point corresponds to Q_{max} and I_{max} measurements from a single oocyte. Oocytes were obtained from several donor frogs over a period of four months.

of substrate fluxes and, in some cases, channel modes of activity have been suggested (Cammack et al., 1994; Mager et al., 1994; Fairman et al., 1995; Galli et al., 1995; Cammack & Schwartz, 1996; Galli, Blakely & DeFelice, 1996; Lin, Lester & Mager, 1996; Sonders & Amara, 1996; Sonders et al., 1997). That the mGAT3 inward charge translocation obtained from the electrophysiological data was directly proportional to GABA influx (2.2 ± 0.1 charges/GABA) suggests that, under these conditions, GABA transport by mGAT3 is tightly coupled to cotransport of ions (Na^+ and Cl^-) with no or insignificant GABA-evoked uncoupled currents.

It has also been observed that some Na^+-coupled transporters exhibit "leak" currents in the presence of Na^+ but in the absence of substrate (Umbach, Coady & Wright, 1990; Sonders & Amara, 1996; Eskandari et al., 1997; Forster et al., 1997; Sonders et al., 1997). For the intestinal Na^+/glucose cotransporter, the leak currents are thought to result from Na^+ translocation mediated by transporter conformational changes (Panayotova-Heiermann et al., 1998; Loo et al., 1999). For rat GAT-1 and the serotonin transporter, the leak currents have been proposed to result from channel activity (Cammack & Schwartz, 1996; Lin et al., 1996). However, GAT1 leak currents have been observed only with the transporter expressed in mammalian cells (Cammack et al., 1994; Cammack & Schwarz, 1996), but not in *Xenopus laevis* oocytes (Lu & Hilgemann, 1999a; Mager et al., 1993). The low turnover rate of mGAT3 (1.7 sec^{-1}) together with the absence of a specific inhibitor, do not allow us to examine this feature with certainty. Experiments are currently under way to address this issue.

Presteady-State Charge Movements

All electrogenic Na^+-coupled transporters examined so far exhibit presteady-state current transients in response to step changes in membrane voltage (e.g., Loo et al., 1993; Mager et al., 1993; Wadiche et al., 1995; Mackenzie et al., 1996; Eskandari et al., 1997; Forster et al., 1998; Forlani et al., 2001b). The charge movements of mGAT3 exhibit similarities to as well as significant differences from those of other Na^+-coupled transporters. For mGAT3, these voltage-induced charge movements are most pronounced at positive membrane potentials. For the ON response, the charge movements exhibit a very fast rising phase (≤2 msec), but the major component of the relaxation can be described by a single exponential function with a time constant of ≤30 msec. The charge-voltage (Q-V) relations are adequately described by a single Boltzmann function suggesting that the process may be approximated as a transition between two states with one dominant voltage-dependent rate-limiting step (Loo et al., 1993). The midpoint of the Q-V curve is at ≈30 mV. It is at around this voltage that the half-maximal concentration for steady-state GABA-evoked currents increases dramatically (Fig. 2*C*). This suggests that large depolarizations reduce the probability that the substrate binding-site faces the external space, and this effect becomes pronounced at potentials greater than ≈30 mV, as at these potentials > 50% of the binding sites are probably not available to bind GABA. Therefore, the Q-V relationship may provide important clues about the accessibility of the binding sites (Li et al., 2000; Loo et al., 1998).

The apparent valence of the moveable charge ($z\delta = 1.6$) obtained from the Boltzmann fit of the Q-V relationship is significantly higher than that reported for GAT-1 and BGT-1 (≈1) (Mager et al., 1993, 1996; Lu & Hilgemann, 1999b; Li et al., 2000; Loo et al., 2000; Forlani et al., 2001a,b), as well as other Na^+-coupled transporters (usually ≤1) (Loo et al., 1993, 1998; Wadiche et al., 1995; Mackenzie et al., 1996; Eskandari et al., 1997; Forster et al., 1997, 1998; Hazama et al., 1997). Thus, the transitions leading to the charge movements of mGAT3 appear to be more voltage-dependent than those of other Na^+-coupled transporters. The data are suggestive of the translocation of two or more elementary charges within the membrane electric field.

Whereas in most transporters examined, the ON and OFF relaxation time constants are within the same order of magnitude, those of mGAT3 do not follow this trend. mGAT3 ON relaxations are similar to those of other transporters. They exhibit a bell-shaped voltage distribution, and the maximum value for τ_{ON} occurs at the same voltage as the $V_{0.5}$ of the Q-V relationship. Manipulations that lead to shifts of the Q-V relationship (e.g., changes in $[Na^+]_o$ or $[Cl^-]_o$) lead to corresponding shifts in the τ_{ON}-V re-

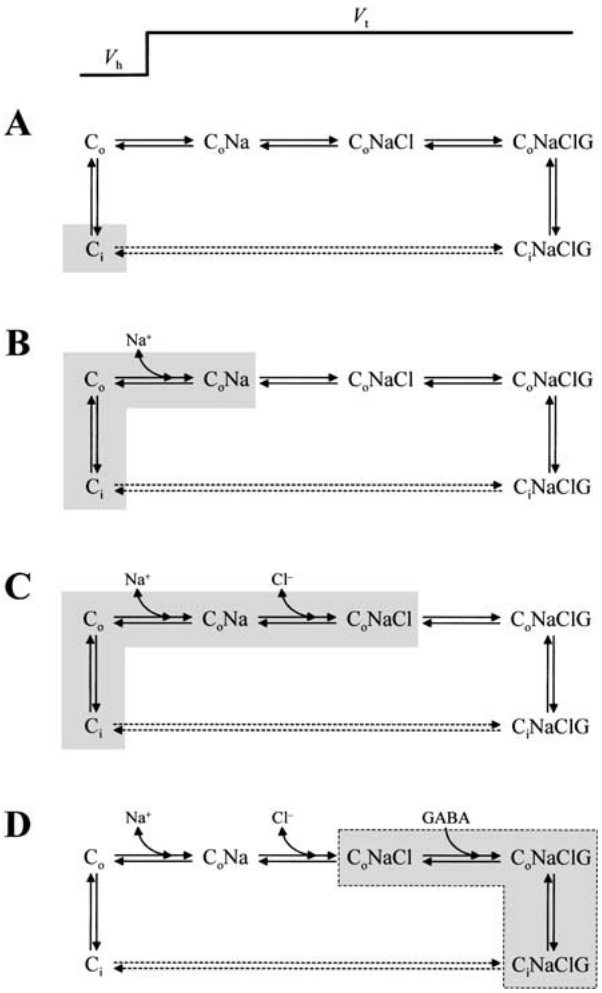

Fig. 13. Interpretation of mGAT3 presteady-state charge movements. Charge movements are seen upon application of voltage pulses (top trace; V_h, holding voltage; V_t, test voltage) (*see* Fig. 4); they are seen in the presence of external Na^+ (Figs. 7 and 10); they are enhanced in the presence of external Cl^- (Fig. 11); and they are completely abolished in the presence of saturating concentrations of GABA (Figs. 7 and 9). *C* denotes carrier (mGAT3); *Na*, Na^+; *Cl*, Cl^-; and *G*, GABA. The subscripts "o" and "i" refer to the outward and inward facing carrier binding sites. No information is available regarding the partial reactions at the cytoplasmic face of the carrier and, therefore, these steps are lumped in one transition represented by the dashed arrows. Shaded regions represent the predominant voltage- and/or GABA-induced transitions under the specified composition of the extracellular solution. (*A*) No Na^+ present. When no external Na^+ is present (even with Cl^- present), the transporter is confined to a state that, in the voltage range tested, does not move charge in response to either depolarizing or hyperpolarizing pulses. (*B*) Na^+ present. In the presence of Na^+ but in the absence of Cl^- and GABA), mGAT3 assumes a Na^+-bound conformation (C_oNa). Voltage pulses induce charge movements. The states responsible for the observed charge movements are shaded. The magnitude of charge obtained under this condition is ≈30% of Q_{max}. At the onset of the pulse, the transitions involve Na^+ dissociation followed by reorientation of the empty transporter. On return to the holding voltage, the steps are reversed. (*C*) Na^+ and Cl^- present. When both Na^+ and Cl^- are present, mGAT3 assumes a conformation most likely to accept GABA. Under these ionic conditions, voltage pulses induce the maximum charge (Q_{max}) obtained. Cl^- itself appears not to contribute to Q_{max}, but it may stabilize the fully Na^+-loaded state. The order of Na^+ and Cl^- binding to the transporter is not known. (*D*) Na^+, Cl^-, and GABA present. With Na^+, Cl^-, and GABA present, no charge movement is observed. The GABA-bound conformational changes (shaded region outlined by a broken line) are either electrically silent or, alternatively, any putative transients associated with these transitions decay too rapidly for detection with the two-electrode voltage-clamp method. The shaded steps correspond to transitions induced by GABA, however, the probability of occupancy of these states is very small, as these appear not to be the rate-limiting steps in the entire transport cycle. The rate-limiting steps for the entire transport cycle appear to be those shaded in panel *C* (clock-wise transitions).

lationship. Thus, the voltage-induced ON transition can be approximated as a two-state process governed by one dominant voltage-dependent rate-limiting step. However, the OFF transients relax very slowly to a steady-state ($\tau_{OFF} \approx 1$ sec). This behavior is unique to mGAT3 and, to our knowledge, has not been observed for any other Na^+-coupled cotransporter. It may have important consequences for the low turnover rate of this transporter (*see* Steady-State Turnover Rate).

Na^+-Cl^-, and GABA Dependence of the Presteady-State Charge Movements

The main advantage of the study of transporter charge movements is that it allows an examination of the partial reactions of the transport cycle (*see* Fig. 13) (Loo et al., 1993, 1998; Mager et al., 1993, 1996; Hazama et al., 1997; Hilgemann & Lu, 1999; Lu & Hilgemann, 1999b; Li et al., 2000). By examining the Na^+, Cl^-, and GABA-dependence of the charge movements, it is possible to infer information regarding the transport cycle, additional to that possible from steady-state measurements alone. Importantly, the Na^+- and Cl^--dependence may be examined in the absence of GABA, and the nature of these interactions may be compared to those for steady-state transport, where these interactions are obligatorily examined in the presence of GABA. The charge movements indicate that Na^+ can interact with the transporter in the absence of both Cl^- and GABA, Cl^- can interact with the transporter in the absence of GABA, and GABA can interact with the transporter in the absence of Cl^-. Because of the strict Na^+-dependence of steady-state transport as well as presteady-state charge movements, it cannot be determined whether Cl^- or GABA can interact with mGAT3 in the absence of Na^+. It has been shown, however, that Cl^- can interact with the cytoplasmic surface of rat GAT-1 in the absence of cytoplasmic Na^+ (Lu et al., 1995; Lu & Hilgemann, 1999a,b).

The charge movements are activated strictly by Na^+, enhanced by Cl^-, and abolished by GABA (Figs.

7, 9–11, and 13). The half-maximal concentration values for Na^+ activation (48 mM) and Cl^- enhancement (19 mM) of the charge movements are considerably higher than the corresponding values for Na^+ activation and Cl^- enhancement of steady-state GABA transport (14 mM and 5 mM, respectively). However, the GABA concentration for 50% elimination of the charge movements (5 μM; Na^+ and Cl^- present) is nearly the same as that for GABA activation of steady-state transport currents (3 μM). These observations suggest that GABA most preferentially interacts with the Na^+- and Cl^--loaded carrier. Importantly, GABA reduces Q_{max} without a change in the voltage distribution of the charge movements (Q-V relationship; Fig. 9*D*), or the relaxation time constants. By binding to the transporter, GABA merely reduces the total number of transporter molecules that are available to move charge. Accordingly, in the presence of GABA, two populations of mGAT3 exist: (*i*) GABA-bound transporters not able to move charge, and (*ii*) transporters without GABA responding to voltage pulses in the same manner as in complete absence of GABA. The relative abundance of each population depends on the GABA concentration.

The above findings may be interpreted in the following manner. Voltage jumps elicit charge movements in the Na^+- and Cl^--loaded carrier (Fig. 13*B* and *C*). GABA binding and/or translocation comprise partial reactions in the transport cycle with very high rates (Fig. 13*D*). Therefore, when GABA binds to a Na^+- and Cl^--loaded carrier molecule, the translocation step follows rapidly (Lester, Cao & Mager, 1996; Mager et al., 1996). Voltage pulses do not elicit charge movements in GABA-loaded carriers because either (*i*) the GABA binding and/or translocation rates are very high, or (*ii*) these transitions are electroneutral (Mager et al., 1993, 1996; Hilgemann & Lu, 1999; Lu & Hilgemann, 1999b). Depolarizing voltage pulses cannot overcome these rates so that charge movements are not observed in the presence of GABA. It is conceivable that extremely large (and/or long) voltage pulses may reveal charge movements in the presence of GABA. However, in the limit of the depolarizing voltages tolerated by oocytes, the rates involving GABA binding and/or translocation of the Na^+/Cl^-/GABA-bound carrier are considerably higher than those giving rise to charge movements ($\tau \leq 30$ msec).

The strict dependence of the charge movements on external Na^+ suggests that they arise from voltage perturbations of the Na^+-loaded carrier (Fig. 13). Na^+ activation of the charge movements follows a sigmoidal relationship with a Hill coefficient of 2.4, hinting at the cooperative interaction of at least two Na^+ ions (even in the absence of GABA). As seen for other electrogenic Na^+-coupled transporters, reductions in $[Na^+]_o$ lead to a shift of the Q-V relationship (≈ -100-mV shift for a 10-fold reduction in Na^+) to negative potentials, and this has been interpreted as a reduction in the accessibility of the Na^+-binding sites from the external space (Loo et al., 1993, 1998, 2000; Mager et al., 1993, 1996; Hazama et al., 1997; Hilgemann & Lu, 1999; Lu & Hilgemann, 1999a,b; Li et al., 2000). Although in the absence of Na^+, increasing the $[Cl^-]_o$ does not lead to detectable charge movements, in the presence of Na^+, external Cl^- enhances Q_{max} by ≈300% (Fig. 11). This behavior is in contrast to that observed for rat (Mager et al., 1993, 1996) and human GAT-1 (Loo et al., 2000), in which no reduction in Q_{max} is observed even at nominal zero $[Cl^-]_o$. If the charge movements represent Na^+ and Cl^- entry/exit into/out of the membrane electric field (*see* Fig. 13), an increase in Q_{max} is expected in the absence of external Cl^- (assuming unaltered Na^+ interaction). In contrast, there is a large reduction (≈70%) in Q_{max} in the absence of external Cl^-.

Furthermore, reductions in both $[Na^+]_o$ and $[Cl^-]_o$ lead to a shift of the Q-V relationship toward negative membrane potentials, whereas based strictly on the ionic nature, opposite effects are expected. The magnitudes of these shifts are similar for mGAT3 and GAT1. Thus, it appears that changes in both $[Na^+]_o$ and $[Cl^-]_o$ ultimately affect similar molecular transitions (as deduced from the decrease in Q_{max} and left-shift of the Q-V curve). The strict dependence of the charge movements on Na^+ suggests that Cl^- binding/dissociation to/from the transporter does not directly contribute to charge movements. Rather, Cl^- either directly or allosterically optimizes Na^+ binding and/or Na^+-induced transporter conformational changes, allowing carrier accumulation in a fully Na^+-loaded state, which can move the maximum amount of charge (Lester et al., 1994; Lu & Hilgemann, 1999b; Mager et al., 1996). That Q_{max} decreases in the nominal absence of Cl^- hints to a reduction in the accessibility of Na^+ binding sites from the external surface. The data still cannot determine whether Cl^- binds before or after Na^+.

It may seem counterintuitive that interaction of an anion with the transporter does not lead to noticeable charge movements. One possibility is that the Cl^- binding site is at or beyond the membrane electric field/water interface such that Cl^- binding/dissociation does not sense the membrane electric field. Alternatively, Cl^- entry into the membrane electric field may occur along a very low access resistance path, and the voltage drop across such a path may be very small to allow for detection of transient currents.

Steady-State Turnover Rate

I_{max} provides a good estimate of the macroscopic rate of transport (*see* Fig. 1*C*), and Q_{max} provides a good estimate of the total number of functional transporters in the plasma membrane (Zampighi et al.,

1995; Eskandari et al., 2000). The ratio of I_{max} to Q_{max} yields the rate of transport per transporter molecule in the plasma membrane (i.e., turnover rate). The turnover rate of mGAT3 was found to be 1.7 sec^{-1} at −50 mV and, consistent with the *I-V* curve (Fig. 1*B*), this value increased to 3.8 sec^{-1} at −150 mV. The turnover rate determined here at −50 mV is lower than that of rat GAT-1 (4–9 sec^{-1}; Mager et al., 1993; Forlani et al., 2001a), human GAT-1 (5 sec^{-1}; Eskandari et al., unpublished), and canine BGT-1 (10 sec^{-1}; Forlani et al., 2001b). The turnover rates of neurotransmitter transporters are considerably lower than those of other Na^+-coupled cotransporters. For cotransporters belonging to the Na^+/glucose cotransporter (SGLT) family, the turnover rate ranges from 20–60 sec^{-1} (at −50 mV) (Mackenzie et al., 1996; Eskandari et al., 1997; Wright et al., 1998).

The low turnover rate of mGAT3 may be explained by the nature of the presteady-state OFF transients upon return to the holding voltage from depolarizing voltage pulses. These steps represent the return of the binding sites to the external medium, Na^+ entry into the membrane electric field, Na^+ binding, and subsequent Na^+-induced conformational changes (Loo et al., 1993, 1998; Mager et al., 1993, 1996; Hilgemann & Lu, 1999; Lu & Hilgemann, 1999b; Li et al., 2000). Our data suggest that these transitions are slow with a time constant of ≈1 sec, predicting a transport cycle rate of ≈1/sec. This is in general agreement with our estimate of the turnover rate (1.7 sec^{-1} at −50 mV). Although it is not known whether during the normal transport cycle, the transporter goes through similar steps as it does in recovery from depolarizing voltage perturbations, some evidence suggests that these transitions represent the rate-limiting steps in the transport cycle. In rat GAT-1, the rate-limiting voltage-dependent step appears to be the same in the absence of GABA as well as for the GABA-loaded transporter, and involves the interaction of Na^+ with the transporter (Mager et al., 1993; Forlani et al., 2001a). Our data suggest that these findings may also hold for mGAT3 (*see* Figs. 9–13). Thus, the slow relaxation of the OFF transients may represent the rate–limiting steps in the transport cycle, leading to the observed low turnover rate of mGAT3.

We thank Michael J. Errico, William Lee, and Erik B. Malarkey for technical assistance. This work was supported by U.S. National Institutes of Health Grants awarded to S.E. (S06 GM53933) and E.M.W. (DK19657 and GM99004), and by grants from the Israel Science Foundation and the United States-Israel Binational Scientific Foundation awarded to N.N.

References

Borden, L.A. 1996. GABA transporter heterogeneity: Pharmacology and cellular localization. *Neurochem. Int.* **29:**335–356

Borden, L.A., Dhar, T.G., Smith, K.E., Branchek, T.A., Gluchowski, C., Weinshank, R.L. 1994. Cloning of the human homologue of the GABA transporter GAT-3 and identification of a novel inhibitor with selectivity for this site. *Receptors Channels* **2:**207–213

Borden, L.A., Smith, K.E., Gustafson, E.L., Branchek, T.A., Weinshank, R.L. 1995. Cloning and expression of a betaine/GABA transporter from human brain. *J. Neurochem.* **64:**977–984

Borden, L.A., Smith, K.E., Hartig, P.R., Branchek, T.A., Weinshank, R.L. 1992. Molecular heterogeneity of the γ-aminobutyric acid (GABA) transport system. Cloning of two novel high affinity GABA transporters from rat brain. *J. Biol. Chem.* **267:**21098–21104

Cammack, J.N., Schwartz, E.A. 1996. Channel behavior in a γ-aminobutyrate transporter. *Proc. Natl. Acad. Sci. USA* **93:**723–727

Cammack, J.N., Rakhilin, S.V., Schwartz, E.A. 1994. A GABA transporter operates asymmetrically and with variable stoichiometry. *Neuron* **13:**949–960

Cao, Y., Li, M., Mager, S., Lester, H.A. 1998. Amino acid residues that control pH modulation of transport-associated current in mammalian serotonin transporters. *J. Neurosci.* **18:**7739–7749

Clark, J.A., Amara, S.G. 1994. Stable expression of a neuronal γ-aminobutyric acid transporter, GAT-3, in mammalian cells demonstrates unique pharmacological properties and ion dependence. *Mol. Pharmacol.* **46:**550–557

Clark, J.A., Deutch, A.Y., Gallipoli, P.Z., Amara, S.G. 1992. Functional expression and CNS distribution of a β-alanine-sensitive neuronal GABA transporter. *Neuron* **9:**337–348

Eskandari, S., Kreman, M., Kavanaugh, M.P., Wright, E.M., Zampighi, G.A. 2000. Pentameric assembly of a neuronal glutamate transporter. *Proc. Natl. Acad. Sci. USA.* **97:**8641–8646

Eskandari, S., Loo, D.D.F., Dai, G., Levy, O., Wright, E.M., Carrasco, N. 1997. Thyroid Na^+/I^- symporter. Mechanism, stoichiometry, and specificity. *J. Biol. Chem.* **272:**27230–27238

Fairman, W.A., Vandenberg, R.J., Arriza, J.L., Kavanaugh, M.P., Amara, S.G. 1995. An excitatory amino-acid transporter with properties of a ligand-gated chloride channel. *Nature* **375:**599–603

Forlani, G., Bossi, E., Ghirardelli, R., Giovannardi, S., Binda, F., Bonadiman, L., Ielmini, L., Peres, A. 2001a. Mutation K448E in the external loop 5 of rat GABA transporter rGAT1 induces pH sensitivity and alters substrate interactions. *J. Physiol.* **536:**479–494

Forlani, G., Bossi, E., Perego, C., Giovannardi, S., Peres, A. 2001b. Three kinds of currents in the canine betaine-GABA transporter BGT-1 expressed in *Xenopus laevis* oocytes. *Biochim. Biophys. Acta* **1538:**172–180

Forster, I., Hernando, N., Biber, J., Murer, H. 1998. The voltage dependence of a cloned mammalian renal type II Na^+/P_i cotransporter (NaP_i-2). *J. Gen. Physiol.* **112:**1–18

Forster, I.C., Wagner, C.A., Busch, A.E., Lang, F., Biber, J., Hernando, N., Murer, H., Werner, A. 1997. Electrophysiological characterization of the flounder type II Na^+/P_i cotransporter (NaP_i-5) expressed in *Xenopus Jaevis* oocytes. *J. Membrane Biol.* **160:**9–25

Gadea, A., López-Colomé, A.M. 2001. Glial transporters for glutamate, glycine, and GABA: II. GABA transporters. *J. Neurosci. Res.* **63:**461–468

Galli, A., Blakely, R.D., DeFelice, L.J. 1996. Norepinephrine transporters have channel modes of conduction. *Proc. Natl. Acad. Sci. USA* **93:**8671–8676

Galli, A., DeFelice, LJ., Duke, B.-J., Moore, K.R., Blakely, R.D. 1995. Sodium-dependent norepinephrine-induced currents in

norepinephrine-transporter-transfected HEK-293 cells blocked by cocaine and antidepressants. *J. Exp. Biol.* **198:**2197–2212

Green, A.R., Hainsworth, A.H., Jackson, D.M. 2000. GABA potentiation: A logical pharmacological approach for the treatment of acute ischaemic stroke. *Neuropharmacology* **39:**1483–1494

Guastella, J., Nelson, N., Nelson, H., Czyzyk, L., Keynan, S., Miedel, M.C., Davidson, N., Lester, H.A., Kanner, B.I. 1990. Cloning and expression of a rat brain GABA transporter. *Science* **249:**1303–1306

Hazama, A., Loo, D.D.F., Wright, E.M. 1997. Presteady-state currents of the rabbit Na^+/glucose cotransporter(SGLT1). *J. Membrane Biol.* **155:**175–186

Hilgemann, D.W., Lu, C.-C. 1999. GAT1 (GABA:Na^+:Cl^-) cotransport function. Database reconstruction with an alternating access model. *J. Gen. Physiol.* **114:**459–475

Hirsch, J.R., Loo, D.D.F., Wright, E.M. 1996. Regulation of the Na^+/glucose cotransporter expression by protein kinases in *Xenopus laevis* oocytes. *J. Biol. Chem.* **271:**14740–14746

Jursky, F., Nelson, N. 1999. Developmental expression of the neurotransmitter transporter GAT3. *J. Neurosci. Res.* **55:**394–399

Kavanaugh, M.P., Arriza, J.L., North, R.A., Amara, S.G. 1992. Electrogenic uptake of γ-aminobutyric acid by a cloned transporter expressed in *Xenopus* oocytes. *J. Biol. Chem.* **267:**22007–22009

Keynan, S., Suh, Y.-J., Kanner, B.L, Rudnick, G. 1992. Expression of a cloned γ-aminobutyric acid transporter in mammalian cells. *Biochemistry* **31:**1974–1979

Läuger, P. 1991. *Electrogenic Ion Pumps*. Sinauer Associates, Inc., Sunderland

Lester, H.A., Cao, Y., Mager, S. 1996. Listening to neurotransmitter transporters. *Neuron* **17:**807–810

Lester, H.A., Mager, S., Quick, M.W., Corey J.L. 1994. Permeation properties of neurotransmitter transporters. *Annu. Rev. Pharmacol. Toxicol.* **34:**219–249

Li, M., Farley, R.A., Lester, H.A. 2000. An intermediate state of the γ-aminobutyric acid transporter GAT1 revealed by simultaneous voltage clamp and fluorescence. *J. Gen. Physiol.* **115:**491–508

Lill, H., Nelson, N. 1998. Homologies and family relationships among Na^+/Cl^- neurotransmitter transporters. *Methods Enzymol.* **296:**425–436

Liman, E.R., Tytgat, J., Hess, P. 1992. Subunit stoichiometry of a mammalian K^+ channel determined by construction of multimeric cDNAs. *Neuron* **9:**861–871

Lin, F., Lester, H.A., Mager, S. 1996. Single-channel currents produced by the serotonin transporter and analysis of a mutation affecting ion permeation. *Biophys. J.* **71:**3126–3135

Liu, Q.-R., López-Corcuera, B., Mandiyan, S., Nelson, H., Nelson, N. 1993. Molecular characterization of four pharmacologically distinct γ-aminobutyric acid transporters in mouse brain. *J. Biol. Chem.* **268:**2106–2112

Liu, Q.-R., Mandiyan, S., Nelson, H., Nelson, N. 1992. A family of genes encoding neurotransmitter transporters. *Proc. Natl. Acad. Sci. USA* **89:**6639–6643

Loo, D.D.F., Eskandari, S., Boorer, K.J., Sarkar, H.K., Wright, E.M. 2000. Role of Cl^- in electrogenic Na^+-coupled cotransporters GAT1 and SGLT1. *J. Biol. Chem.* **275:**37414–37422

Loo, D.D.F., Hazama, A., Supplisson, S., Turk, E., Wright, E.M. 1993. Relaxation kinetics of the Na^+/glucose cotransporter. *Proc. Natl. Acad. Sci. USA* **90:**5767–5771

Loo, D.D.F., Hirayama, B.A., Gallardo, E.M., Lam, J.T., Turk, E., Wright, E.M. 1998. Conformational changes couple Na^+/and glucose transport. *Proc. Natl. Acad. Sci. USA* **95:**7789–7794

Loo, D.D.F., Hirayama, B.A., Meinild, A.-K., Chandy, G., Zeuthen, T., Wright, E.M. 1999. Passive water and ion transport by cotransporters. *J. Physiol.* **518:**195–202

López-Corcuera, B., Liu, Q.-R., Mandiyan, S., Nelson, H., Nelson, N. 1992. Expression of a mouse brain cDNA encoding novel γ-aminobutyric acid transporter. *J. Biol. Chem.* **267:**17491–17493

López-Corcuera, B., Martínez-Maza, R., Núñez, E., Roux, M., Supplisson, S., Aragón, C. 1998. Differential properties of two stably expressed brain-specific glycine transporters. *J. Neurochem.* **71:**2211–2219

Lu, C.-C., Hilgemann, D.W. 1999a. GAT1 (GABA:Na^+:Cl^-) cotransport function. Steady state studies in giant *Xenopus* oocyte membrane patches. *J. Gen. Physiol.* **114:**429–444

Lu, C.-C., Hilgemann, D.W. 1999b. GAT1 (GABA:Na^+:Cl^-) cotransport function. Kinetic studies in giant *Xenopus* oocyte membrane patches. *J. Gen. Physiol.* **114:**445–457

Lu, C.-C, Kabakov, A., Markin, V.S., Mager, S., Frazier, G.A., Hilgemann, D.W. 1995. Membrane transport mechanisms probed by capacitance measurements with megahertz voltage clamp. *Proc. Natl. Acad. Sci. USA* **92:**11220–11224

Mackenzie, B., Loo, D.D.F., Fei, Y.-J., Liu, W., Ganapathy, V., Leibach, F.H., Wright, E.M. 1996. Mechanisms of the human intestinal H^+-coupled oligopeptide transporter hPEPT1. *J. Biol. Chem.* **271:**5430–5437

Mackenzie, B., Loo, D.D.F., Wright, E.M. 1998. Relationships between Na^+/glucose cotransporter (SGLT1) currents and fluxes. *J. Membrane Biol.* **162:**101–106

Mager, S., Kleinberger-Doron, N., Keshet, G.I., Davidson, N., Kanner, B.I., Lester, H.A. 1996. Ion binding and permeation at the GABA transporter GAT1. *J. Neurosci.* **16:**5405–5414

Mager, S., Min, C., Henry, D.J., Chavkin, C., Hoffman, B.J., Davidson, N., Lester, H.A. 1994. Conducting states of a mammalian serotonin transporter. *Neuron* **12:**845–859

Mager, S., Naeve, J., Quick, M., Labarca, C., Davidson, N., Lester, H.A. 1993. Steady states, charge movements, and rates for a cloned GABA transporter expressed in *Xenopus* oocytes. *Neuron* **10:**177–188

Matskevitch, I., Wagner, C.A., Stegen, C., Bröer, S., Noll, B., Risler, T., Kwon, H.M., Handler, J.S., Waldegger, S., Busch, A.E., Lang, F. 1999. Functional characterization of the betaine/γ-aminobutyric acid transporter BGT-1 expressed in *Xenopus* oocytes. *J. Biol. Chem.* **274:**16709–16716

Nelson, N. 1998. The family of Na^+/Cl^- neurotransmitter transporters. *J. Neurochem.* **71:**1785–1803

Nelson, H., Mandiyan, S., Nelson, N. 1990. Cloning of the human brain GABA transporter. *FEBS Lett.* **269:**181–184

Panayotova-Heiermann, M., Loo, D.D.F., Lam, J.T., Wright, E.M. 1998. Neutralization of conservative charged transmembrane residues in the Na^+/glucose cotransporter SGLT1. *Biochemistry* **37:**10522–10528

Pastuszko, A., Wilson, D.F., Erecinska, M. 1982. Energetics of γ-aminobutyrate transport in rat brain synaptosomes. *J. Biol. Chem.* **257:**7514–7519

Reizer, J., Reizer, A., Saier, M.H. Jr. 1994. A functional superfamily of sodium/solute symporters. *Biochim. Biophys. Acta* **1197:**133–166

Roettger, V.R., Amara, S.G. 1999. GABA and glutamate transporters: Therapeutic and etiologic implications for epilepsy. *Adv. Neurol.* **79:**551–560

Schachter, S.C. 1999. A review of the antiepileptic drug tiagabine. *Clin. Neuropharmacol.* **22:**312–317

Sonders, M.S., Amara, S.G. 1996. Channels in transporters. *Curr. Opin. Neurobiol.* **6:**294–302

Sonders, M.S., Zhu, S.-J., Zahniser, N.R., Kavanaugh, M.P., Amara, S.G. 1997. Multiple ionic conductances of the human dopamine transporter: The actions of dopamine and psychostimulants. *J. Neurosci.* **17:**960–974

Umbach, J.A., Coady, M.J., Wright, E.M. 1990. Intestinal Na^+/glucose cotransporter expressed in *Xenogus* oocytes is electrogenic. *Biophys. J.* **57:**1217–1224

Wadiche, J.I., Arriza, J.L., Amara, S.G., Kavanaugh, M.P. 1995. Kinetics of a human glutamate transporter. *Neuron* **14:**1019–1027

Wright, E.M., Loo, D.D.F., Panayotova-Heiermann, M., Hirayama, B.A., Turk, E., Eskandari, S., Lam, J.T. 1998. Structure and function of the Na^+/glucose cotransporter. *Acta Physiol. Scand.* **163** (*Suppl.* **643**):257–264

Yamauchi, A., Uchida, S., Kwon, H.M., Preston, A.S., Robey, R.B., Garcia-Perez, A., Burg, M.B., Handler, J.S. 1992. Cloning of a Na^+- and Cl^--dependent betaine transporter that is regulated by hypertonicity. *J. Biol. Chem.* **267:**649–652

Zampighi, G.A., Kreman, M., Boorer, K.J., Loo, D.D.F., Bezanilla, F., Chandy, G., Hall, J.E., Wright, E.M. 1995. A method for determining the unitary functional capacity of cloned channels and transporters expressed in *Xenopus laevis* oocytes. *J. Membrane Biol.* **148:**65–78